



Molecular Crystals and Liquid Crystals Science and Technology. Section A. Molecular Crystals and Liquid Crystals

Publication details, including instructions for authors and subscription information:
<http://www.tandfonline.com/loi/gmcl19>

Anomalies within Alkyl and Alkoxy Substituted Bis (1,3-diphenylpropane - 1,3 dionato) Copper (II) metallomesogens from X-ray and EPR Studies

Monisha Bose ^a, Kazuchika Ohta ^b, Tosio Sakurai ^c & Chanchal K. Majumdar ^a

^a S. N. Bose National Centre for Basic Sciences, Block JD, Sector III, Salt Lake, Calcutta, 700091, India

^b Dept. of Functional Polymer Science, Faculty of Textile Science and Technology, Shinshu University, UEDA 386, Japan

^c Department of Science, Faculty of Education, Shinsu University, Nagano, 381, Japan

Version of record first published: 24 Sep 2006

To cite this article: Monisha Bose, Kazuchika Ohta, Tosio Sakurai & Chanchal K. Majumdar (1999): Anomalies within Alkyl and Alkoxy Substituted Bis (1,3-diphenylpropane - 1,3 dionato) Copper (II) metallomesogens from X-ray and EPR Studies, *Molecular Crystals and Liquid Crystals Science and Technology. Section A. Molecular Crystals and Liquid Crystals*, 326:1, 229-247

To link to this article: <http://dx.doi.org/10.1080/10587259908025417>

PLEASE SCROLL DOWN FOR ARTICLE

Full terms and conditions of use: <http://www.tandfonline.com/page/terms-and-conditions>

This article may be used for research, teaching, and private study purposes. Any substantial or systematic reproduction, redistribution, reselling, loan, sub-licensing, systematic supply, or distribution in any form to anyone is expressly forbidden.

The publisher does not give any warranty express or implied or make any representation that the contents will be complete or accurate or up to date. The accuracy of any instructions, formulae, and drug doses should be independently verified with primary sources. The publisher shall not be liable for any loss, actions, claims, proceedings, demand, or costs or damages whatsoever or howsoever caused arising directly or indirectly in connection with or arising out of the use of this material.

Anomalies within Alkyl and Alkoxy Substituted Bis(1,3-diphenylpropane - 1,3 dionato) Copper(II) metallomesogens from X-ray and EPR Studies

MONISHA BOSE^{a,*}, KAZUCHIKA OHTA^b, TOSIO SAKURAI^c
and CHANCHAL K. MAJUMDAR^a

^a S. N. Bose National Centre for Basic Sciences, Block JD, Sector III, Salt Lake,
Calcutta-700091, India;

^b Dept. of Functional Polymer Science, Faculty of Textile Science and Technology,
Shinshu University, UEDA 386, Japan;

^c Department of Science, Faculty of Education, Shinsu University, Nagano 381, Japan

(Received 9 September 1997; In final form 15 June 1998)

Our previous EPR studies dealt with the contrasting behaviour of the lamellar C_8OCu , as against the columnar $C_8Cu/C_{10}Cu$. X-ray and EPR studies of C_nCu ($n = 6 - 12$) and C_nOCu ($n = 6 - 12$) presented here, however, indicate that some members exhibit anomalous behaviour within each series. Thus C_6Cu , C_8Cu , $C_{10}Cu$ and $C_{12}Cu$ (even members) show a single exchange-narrowed strong asymmetric g_{\perp} along with a weak g_{\parallel} in pure solids. Interestingly, C_7Cu and C_9Cu (odd members) show hyperfine quartets in g_{\parallel} , indicating weak or no exchange. C_7Cu shows a single g_{\perp} , conforming to the axial symmetry in C_nCu . However, C_9Cu is rather unique : gives three different mesophases and exhibits non-axial behaviour. Crystal structure for C_6Cu and C_7Cu reported here for the first time, indicate that the former has a structure similar to that of C_8Cu . However, C_7Cu , which also has $z = 1$ and belongs to the same triclinic space group, has a close interaction between two molecules at the opposite corners of the ab plane in the unit cell, through chain-chain intermolecular interaction and possibility $\pi - \pi$ interaction among phenyl-rings in adjacent molecules. This is reflected in the 'c' parameter, which is 10.066 Å, as compared to 5.863 Å in C_6Cu . However, this interaction in C_7Cu vanishes in the mesophase, as indicated by the collapse of the quartet. Weak exchange in C_7Cu is also reflected in the proton relaxation time T_1 (68.9 msec), as compared 1.9 msec for C_6Cu . In C_nOCu , C_7OCu behaves like the dimer C_8OCu , with a complex hyperfine structure including quadrupole forbidden transitions after g_1 , along with a broad g_2 and a weak g_3 . The dimer in C_8OCu is strong and the quartet persists in the mesophase. Other members, possibly monomers *viz.*, C_6OCu , and $C_{10}OCu$, give a hyperfine quartet in g_1 (while in $C_{12}OCu$ it is after g_1),

*Corresponding author. Tel.: 321-5705-10, Fax: 91-33-334-3477, e-mail: root@bose.ernet.in

followed by a strong single g_2 line and a weak g_3 , conforming to the non-axial symmetry of the lamellar complex. Thus, chain length does play a role but not in a linear fashion, because of the anomalies presented above.

Keywords: Copper metallomesogen; X-ray; EPR

1. INTRODUCTION

The first paramagnetic disc-like metallomesogen bis[1,3-di(*p*-*n*-decylphenyl) propane-1,3 dionato] copper(II) was reported by Giroud-Godquin and Billard [1]. Levelut [2] from X-ray studies of this compound (abbreviated as $C_{10}Cu$), considered it to have a lamellar phase with imperfect crystalline organisation. Billard [3] concluded from polarizing microscopic observations that the mesophase of $C_{10}Cu$ has both a columnar and layered (lamellar) structure. From binary phase diagram studies of the homologues *viz.*, C_8Cu and $C_{10}Cu$ and the corresponding alkoxy complex C_8OCu , Ohta *et al.* [4, 5] showed that each of these exhibit mesomorphic phases. C_8Cu had two different mesophases D_1 and D_2 . The latter phase in C_8Cu is the same mesophase of Giroud-Godquin and Billard, while the D phase in C_8OCu was completely miscible with the D_1 Phase of C_8Cu . Further, Ohta *et al.* [6] and Sakashita *et al.* [7] revealed from X-ray studies, that the D mesophase in C_nOCu has a lamellar structure without columnar stacking and the molecules tilt 5° to the layer. Ohta *et al.*, denoted these D_1 and D_2 phases as D_{L1} (discotic lamellar mesophases without columnar structure) and D_{L2} (discotic lamellar mesophases with columnar structure). Thus, these D_{L1} and D_{L2} mesophases are very unique and different from conventional discotic columnar and smectic mesophases.

To study the effect of chain length on mesomorphic properties, Ohta *et al.* [6, 8] had synthesised the whole series of C_nCu and C_nOCu complexes (Fig. 1) from $n = 0-12$, most of which showed two solid polymorphs. Recently, Usha *et al.* [9] have shown that C_8Cu also exhibits two solid polymorphs (needle-like and prismatic) with very different crystal structures. Only $C_{12}Cu$, first reported by Giroud-Godquin *et al.* [10] does not exhibit any polymorphism. In the C_nCu series, complexes from $n = 4-12$ were found to be mesogenic. Some members show plural mesophases *viz.*, C_7Cu and C_8Cu show two different mesophases D_1 and D_2 , whereas C_9Cu shows three mesophases D_1 , D_2 and D_3 . Ohta *et al.* [8] have shown that the textures of D_1 and D_2 phases are the same in C_7Cu and C_8Cu . D_1 in C_8Cu gave a 'plane' texture surrounded by a lustrous ring. In D_2 , this structure got wrinkled. C_9Cu was exceptional with three mesophases : D_1 showed a spiral

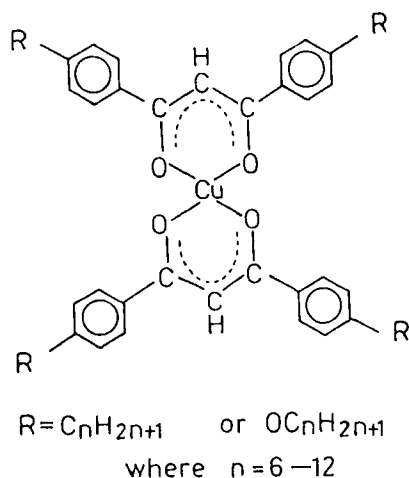


FIGURE 1 Structure of alkyl/alkoxy substituted aryl β diketonates of Cu(II).

texture, which was destroyed in D_2 to give a mosaic texture, surrounded by a lustrous ring. In D_3 , this ring began to be distorted [8] and the mosaic texture began to wrinkle. Thus within this series, the properties differ greatly and abruptly.

In Comparison, C_nOCu appears to be less complex. Thus, all the mesogens from $n = 6 - 12$ give a single mesophase [6], with big broken fan-like texture. Unlike the C_nCu series, the crystal shape is rod-like for $C_6OCu(K_2)$, $C_7OCu(K_2)$ and $C_8OCu(K_3)$ but plate-like for $C_9OCu(K_3)$, $C_{10}OCu$ and $C_{11}OCu$. However, $C_{12}OCu$ is needle-like as in C_nCu . All of them give a lamellar mesophase (D_{L1}), inspite of differences in their molecular shape and may be in crystal structure. Except for C_8OCu , crystal structures of C_nOCu complexes could not be determined, as single crystals could not be grown. Each of the complexes from C_6OCu to $C_{12}OCu$ could easily afford a supercooled discophase at room temperature, which indicates, that this phase (D_{L1}) in C_nOCu has a rather stable structure, and possibly is the reason, why C_nOCu does not have any plural mesophase.

The point to note is that in both the series, though the different polymorphs of a complex give different crystal structures having different melting points (MP), they give the same mesophase. The transition from K to the discotic mesophase involves a significant enthalpy change (ΔH). In the C_nCu series, enthalpy for melting is larger than the enthalpy for clarification, but in C_8OCu , the enthalpy of clarification is higher than that

TABLE I Phase Transition Temperatures (T_i) and enthalpy changes (ΔH_i) n versus $T_i(^{\circ}\text{C})/\Delta H_i(\text{kcal/mol})$

Columnar $C_n\text{Cu}$ ($n = 6-12$)	Mesophase	Lamellar $C_n\text{OCu}$ ($n = 6-12$)
$C_6\text{Cu}(\text{K}_1) \xrightarrow[13.4]{79.3} D \xrightarrow[6.33]{134.0} IL$ $(\text{K}_2) \xrightarrow[5.55]{91.8}$	One	$C_6\text{OCu}(\text{K}_2) \xrightarrow[3.2]{152.9} D \xrightarrow[15.3]{182.4} IL$ $(\text{K}_1) \xrightarrow[1.0]{125.7}$
$C_7\text{Cu}(\text{K}_2) \xrightarrow[13.71]{76.2} D_1 \xrightarrow[0.84]{94.6} D_2 \xrightarrow[6.92]{150.0} IL$ $(\text{K}_1) \xrightarrow[53.9]{}$	Two	$C_7\text{OCu}(\text{K}_2) \xrightarrow[12.8]{111.2} D \xrightarrow[12.1]{180.8} IL$ $(\text{K}_1) \xrightarrow[5.9]{93.9}$
$C_8\text{Cu}(\text{K}) \xrightarrow[26.80]{76.1} D_1 \xrightarrow[0.76]{117.2} D_2 \xrightarrow[8.60]{141.6} IL$	Two	$C_8\text{OCu}(\text{K}_3) \xrightarrow[14.0]{93.1} D \xrightarrow[16.6]{173.3} IL$ $(\text{K}_1) \xrightarrow[0.79]{21.8} (\text{K}_2) \xrightarrow[2.89]{82.5}$
$C_9\text{Cu}(\text{K}_1) \xrightarrow[21.66]{68.0} D_1 \xrightarrow[1.20]{99.8} D_2 \xrightarrow[0.49]{111.1} D_3 \xrightarrow[7.47]{137.0} IL$ $(\text{K}_2) \xrightarrow[5.39]{82.6}$	Three	$C_9\text{OCu}(\text{K}_3) \xrightarrow[25.9]{94.5} D \xrightarrow[14.49]{170.7} IL$ $(\text{K}_1) \xrightarrow[3.1]{55.6} (\text{K}_2) \xrightarrow[0.5]{84.2}$
$C_{10}\text{Cu}(\text{K}_2) \xrightarrow[29.50]{91.3} D \xrightarrow[7.71]{130.1} IL$ $(\text{K}_1) \xrightarrow[21.67]{86.0}$	One	$C_{10}\text{OCu}(\text{K}) \xrightarrow[10.9]{81.9} D \xrightarrow[15.1]{166.6} IL$
$C_{11}\text{Cu}(\text{K}_1) \xrightarrow[8.54]{84.2} D \xrightarrow[125.3]{148.8} IL$ $(\text{K}_2) \xrightarrow[96.6]{}$	One	$C_{11}\text{OCu}(\text{K}) \xrightarrow[26.8]{87.6} D \xrightarrow[14.8]{161.2} IL$
$C_{12}\text{Cu}(\text{K}) \xrightarrow[34.76]{98.9} D \xrightarrow[7.35]{119.8} IL$	One	$C_{12}\text{OCu}(\text{K}) \xrightarrow[29.4]{74.3} D \xrightarrow[12.4]{154.1} IL$

of fusion, which is a rare situation for organic discogens, first reported by Fugnitto *et al.* [11]. However in C_8OCu , this situation is now understandable from Usha *et al.*'s [12] crystallographic studies. In this compound, the repeating unit is a dimer with $z = 2$, as against the monomer in C_8Cu with $z = 1$. The strong bond in the dimer persists in the mesophase (high enthalpy not required) but is broken only in the isotropic phase (higher enthalpy required), as has been shown from EPR [15].

Eastman *et al.* [13] first reported that single crystals of C_8Cu show a single exchange-narrowed EPR line in X-band at room temperature. He considered C_8Cu to be a one-dimensional Heisenberg antiferromagnet and could observe the phase transition from K to the D_1 phase. The change in spectrum was observable, but not dramatic, as exchange effects still persisted in the mesophase. In C_8OCu , they did not see the exchange-narrowed line but observed a complex spectrum with a hyperfine structure. No spectrum of C_8OCu was presented and no further work was reported. This motivated Bose and Sadashiva [14, 15] to pursue a thorough study of this contrasting behaviour between alkyl and alkoxy substitution in aryl β diketonates of Cu from X band and Q band EPR. Their early 1H NMR studies [14] in $C_{10}Cu$ and C_8OCu , though confirmed fluidity in these discogens, failed to distinguish between columnar $C_{10}Cu$ and lamellar C_8OCu . However, they have shown from magnetic susceptibility studies [16] that Eastman's contention of C_8Cu being a spin 1/2 one dimensional Heisenberg antiferromagnet at room temperature is not true, as C_8Cu fails to order even at liquid helium temperatures. But the strong antiferromagnetic exchange ($J_{ex} \gg A$) in $C_8Cu/C_{10}Cu$ is confirmed from the strong exchange-narrowed asymmetric g_{\perp} line (14), along with a very weak g_{\parallel} (axially symmetric). C_8OCu in the Q band on the other hand, clearly revealed a complex hyperfine pattern [15] after a weak g_1 , along with a wide (140 Oe) g_2 line and a weak g_3 , indicating a non-axial system, with weak or no exchange-narrowing ($J_{ex} \ll A$). Thus C_8Cu EPR, conformed to the axial columnar system and C_8OCu to the non-axial staggered lamellar structure, as reported in X-ray studies by Usha *et al.* [12, 17]. Q band spectra of C_8OCu , indicated the presence of quadrupole forbidden transitions [18], along with the Cu hyperfine quartet from the distorted dimer of C_8OCu , the repeating unit in the unit cell. The copper ion was not on an inversion centre, as in C_8Cu , but in a zig-zag configuration, with Cu-Cu distances alternating between 6.3 and 6.6 Å. The existence of quadrupolar forbidden transition has been confirmed by a computer simulation of the hyperfine spectrum and good agreements between line positions and intensities were obtained from C_8OCu and the mixed complex $2C_8Cu-2OC_8$ [16].

However, when C_8Cu and $C_{10}Cu$ were doped into the corresponding Pd complex, the weak g_{\parallel} splitted up to give a hyperfine quartet, in which the outer lines suffered isotopic splitting in the ratio of 1 : 2, due to presence of ^{35}Cu and ^{37}Cu in that ratio [19]. The corresponding g_{\perp} line gave a hyperfine structure with Cu quartet and quadrupole forbidden transitions in place of the single exchange-narrowed line. Similar spectra were obtained with $C_8Cu/C_{10}Cu$ in frozen chloroform solution. Thus, at the molecular level, C_8Cu and C_8OCu behave in the same fashion. However, in the solid, packing effects dominate. C_8Cu with Cu–Cu distances at 5.82 Å gives a one-dimensional close-packed columnar structure, wherein strong exchange-interaction wipe out any fine structure, whereas in C_8OCu , the bulky alkoxy group lead to a staggered two-dimensional lamellar structure with Cu–Cu distances > 6 Å, leading to absence of long-range exchange-interaction effects.

In the present paper, X-ray and EPR studies have been extended to cover the two entire series, C_nCu and C_nOCu , in an effort to unravel any correlation which may exist between polymorphism, plural mesophase formation, texture and crystal structure with changes in chain length across the series.

2. EXPERIMENTAL

2.1. Preparation of the Cu Complexes

Both the series, C_nCu and C_nOCu complexes were prepared according to Ohta *et al.*'s original publications [6, 8]. In C_nCu homologous series, the virgin crystals obtained by recrystallisation from organic solvent gave needle-like or cotton like crystals. However, the crystalline C_7Cu was obtained as flakes, which are totally different from the others.

2.2. X-ray Studies

Diffraction data on single crystals of C_6Cu (needle-like) and C_7Cu (flake-like) were collected at room temperature using a Rigaku AFC-5S four circle diffractometer with $M_o - K_{\alpha}$ radiation. Single crystals of C_6Cu and C_7Cu , former recrystallised from ethyl acetate and the latter from hexane having the dimensions $0.28\text{ mm} \times 0.16\text{ mm} \times 1.00\text{ mm}$ and $0.36\text{ mm} \times 0.02\text{ mm} \times 1.00\text{ mm}$ respectively were used. Attempts at growing other crystals (other than $C_8Cu/C_8OCu/C_{10}Cu$ studied by Usha *et al.*) of the C_nCu/C_nOCu series were not successful.

2.3. EPR Spectra

X and Q Band Spectra of the virgin samples (powders) were recorded with a Varian E 112 Spectrometer along with E 257 Variable temperature accessory.

3. RESULTS AND DISCUSSION

3.1. X-ray Work on C_6Cu and C_7Cu

Tables II and III give the crystal data on the two complexes and Figures 2 and 3 give the molecular arrangements in the *ab* plane. Though C_7Cu differs from C_6Cu by a single CH_2 group and belongs to the same triclinic space group $P\bar{1}$ with $Z = 1$, the crystal structures and molecular arrangements are very different. Thus as seen from Tables II and III, '*c*' axis in C_6Cu has a value of 5.863 Å, whereas in C_7Cu , the value is almost double ~ 10.066 Å. Further, Figures 2 and 3 indicate that the molecular arrangements in '*ab*' plane are very different, leading to an open structure in C_6Cu (similar to Usha's C_8Cu) but a rather crowded structure in C_7Cu . In C_6Cu , the molecules are more or less parallel to the *ab* plane with the alkyl chains in an all trans configuration. Further, there is no interaction between the organic groups *viz.*, phenyl-chain, chain-chain, phenyl-phenyl *etc.*, except the magnetic exchange interaction between Cu^{2+} ions on the inversion centre, along a column where Cu-Cu separation is ~ 5.863 Å. But in C_7Cu , the molecules are not parallel to the '*ab*' plane but the phenyl rings with the chains tilt substantially from the '*ab*' plane, causing the distance between two successive layers to increase, as observed. Of the four alkyl chains, only two are in an all trans form, while rest of the chains contain a cis part (circled in Fig. 3). Moreover, the stacking in the layer along '*ab*' (2d) results in a very close interaction with the chains of a molecule in one corner with the chains of the molecule in the opposite corner of the unit cell. Further, four phenyl rings of two neighbouring molecules pile up along the *b* direction, possibly close enough (separation ~ 4.4 Å) for π - π interaction as shown in Figure 3. Thus the molecules are not free in the '*ab*' plane but are clubbed together forming interacting pairs. Thus C_7Cu behaves differently, as columnar stacking in the '*c*' direction is not possible, leading to an increase in the Cu-Cu distance (~ 10.066 Å), as compared to that in C_6Cu . However, though the coordination around Cu is basically square planar in both C_7Cu and C_6Cu , the phenyl rings along with alkyl chains are severely distorted.

TABLE II Crystal data for C₆Cu

1.	Empirical Formula	C(54)H(70)O(4)Cu(1)
2.	Formula Weight	846.69
3.	Crystal System	Triclinic
4.	Lattice Parameters	$a = 14.171$ (6) angstroms $b = 15.358$ (4) angstroms $c = 5.863$ (3) angstroms $\alpha = 95.20$ (3) degrees $\beta = 93.15$ (5) degrees $\gamma = 109.88$ (3) degrees $V = 1190.0$ (8) angstroms ³
5.	Space Group	P-1(#2)
6.	Z Value	1
7.	Dcalc	1.18 g/cm ³
8.	FOOO	455
9.	μ (Mo K-alpha)	5.00 cm ⁻¹
10.	Diffractometer	Rigaku AFC5S
11.	Radiation	Mo K-alpha ($\lambda = 0.71069$) Graphite-Monochromated
12.	Temperature	23 degrees Cent.
13.	2-theta (max)	55.0 degrees
14.	No. Observations ($I > 3.00$ (sig (I)))	3130
15.	No. Variables	268
16.	Residuals: R; Rw	0.046; 0.056
17.	Goodness of Fit Indicator	1.25
18.	Maximum Shift in Final Cycle	1.36
19.	Largest Peak in Final Diff. Map	0.56 e/angstrom ³

TABLE III Crystal data for C₇Cu

1.	Empirical Formula	C(58)H(78)O(4)Cu(1)
2.	Formula Weight	902.80
3.	Crystal System	Triclinic
4.	Lattice Parameters	$a = 10.316$ (6) angstroms $b = 13.326$ (7) angstroms $c = 10.066$ (7) angstroms $\alpha = 90.77$ (6) degrees $\beta = 92.71$ (7) degrees $\gamma = 71.25$ (4) degrees $V = 1309$ (1) angstroms ³
5.	Space Group	P-1(#2)
6.	Z Value	1
7.	Dcalc	1.15 g/cm ³
8.	FOOO	487
9.	μ (Mo K-alpha)	4.58 cm ⁻¹
10.	Diffractometer	Rigaku AFC5S
11.	Radiation	Mo K-alpha ($\lambda = 0.71069$) Graphite-monochromated
12.	Temperature	23 degrees Cent.
13.	2-theta(max)	55.0 degrees
14.	No. Observations ($I > 3.00$ (sig (I)))	1477
15.	No. variables	286
16.	Residuals: R; Rw	0.056; 0.064
17.	Goodness of Fit Indicator	1.27
18.	Maximum Shift in Final Cycle	1.09
19.	Largest Peak in Final Diff. Map	0.53 e/angstrom ³

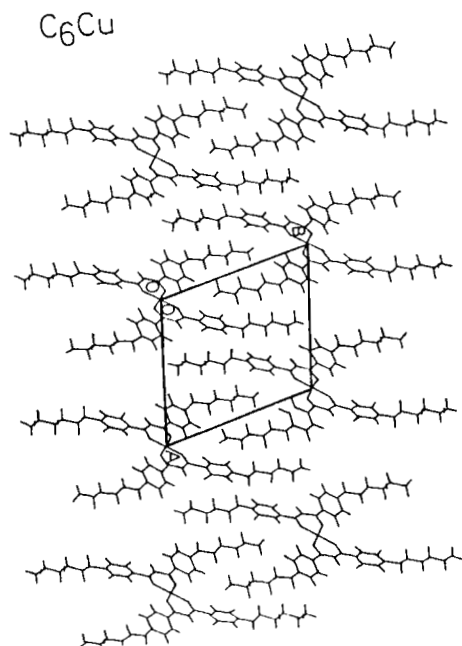


FIGURE 2 Molecular arrangement in the ab plane for C_6Cu .

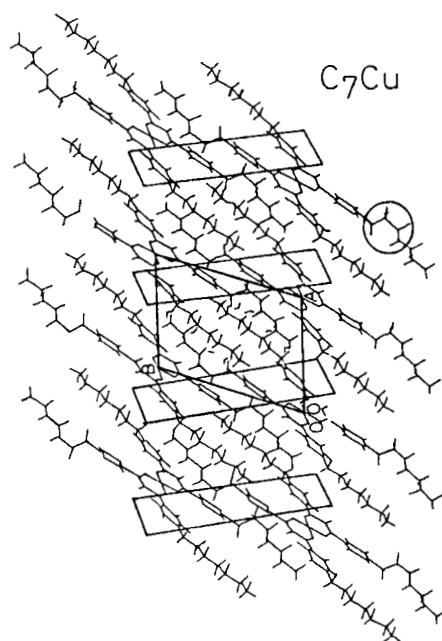


FIGURE 3 Molecular arrangement in the ab plane for C_7Cu .

It has already been pointed out that Usha *et al.* [9] succeeded in obtaining two different crystallographic forms of C_8Cu viz., the more abundant needle-like form and the prismatic form ($Cu-Cu$ distance $\sim 10.34 \text{ \AA}$) having different crystal structures. It appears that C_7Cu has crystal parameters close to that of prismatic C_8Cu (Tab. IV), which again has been shown to be isomorphous with $C_{10}Pd$ with a $Pd-Pd$ distance $\sim 10.26 \text{ \AA}$ [20]. However, due to non-availability of sufficient quantity of prismatic crystals, its properties could not be studied. In Table V are listed the average values of the bond lengths and valence angles characterizing the cores. No big difference can be seen from $C_6Cu(K_1)$, $C_7Cu(K_2)$, $C_8Cu(N)$ and $C_8Cu(P)$. The core complex part CuO_4 is completely planar. However, the torsion angles $O-Cu-O-C$ are $+3.1^\circ$ and -3.1° . Hence the ligand part of the core bis (propane-1, 3-dionato) $Cu(II)$ tilts up on one side and down on the other, to give an almost flat chair form.

4. EPR STUDIES AT X AND Q BANDS

EPR studies are recommended to be carried out at two different frequencies to arrive at the correct parameters. Classically EPR spectra was taken in the

TABLE IV Crystal data for C_nCu

		$C_6-Cu(K_1)$	$C_7-Cu(K_2)$	$C_8-Cu(N)^*$	$C_8-Cu(P)^*$
<i>a</i>	Angstroms	14.171(6)	10.316(6)	14.332(1)	11.621(2)
<i>b</i>	Angstroms	15.358(4)	13.326(7)	17.603(2)	12.817(2)
<i>c</i>	Angstroms	05.863(3)	10.066(7)	05.821(3)	10.341(3)
α	Degrees	95.20(3)	90.77(6)	98.86(2)	92.73(2)
β	Degrees	90.15(7)	90.71(7)	93.58(3)	109.55(2)
γ	Degrees	109.88(3)	71.25(4)	107.35(1)	103.99(1)
Space Group		$P\bar{1}$	$P\bar{1}$	$P\bar{1}$	$P\bar{1}$
<i>z</i>	1	1	1	1	1

* Ref. [23].

TABLE V Average dimensions of the core

	$C_6-Cu(K_1)$	$C_7-Cu(K_2)$	$C_8-Cu(N)^*$	$C_8-Cu(P)^*$
$Cu-O/\text{\AA}$	1.905(2)	1.891(0)	1.908(6)	1.90(1)
$O-C/\text{\AA}$	1.276(3)	1.281(4)	1.27(1)	1.27(2)
$C-C/\text{\AA}$	1.394(4)	1.37(6)	1.389(2)	1.38(3)
$O-Cu-O/^\circ$	92.87(9)	92.9(2)	92.8(2)	92.3(2)
$Cu-O-C/^\circ$	126.6(6)	126.7(8)	126.3(4)	127.2(2)
$O-C-C/^\circ$	124.5(3)	124.3(3)	125.0(2)	124.2(4)
$C-C-C/^\circ$	124.2(3)	124.2(3)	124.2(6)	124.4(6)

* Ref. [23].

X band (9 GHz) for small molecules (inorganic and free radicals). But when signals were weak and proper resolution of the lines were not obtained, one went in for the Q band (35 GHz). At this higher frequency, not only were the lines more intense but also due to the spread out of the spectrum, many overlapping lines were clearly separated. In the present work also, $C_n\text{Cu}/C_n\text{OCu}$ were first studied in the X band. In case of $C_8\text{Cu}/C_{10}\text{Cu}$, g_{\parallel} was very weak but somewhat stronger in Q band. The exchange-narrowed g_{\perp} line was reasonably strong but was not much affected by change in frequency from X to Q band. However, in $C_8\text{OCu}$ (complex hyperfine structure), though more lines than the hyperfine quartet were evident in X band, they could not be resolved. But in Q band, the result was remarkable, with the overlapping lines separating out [15], which led to the inference that one was dealing with quadrupole forbidden transitions (q.f.t.), which was finally corroborated by computer simulation [16]. More recently, for large biological molecules, it has been seen [21] that somewhat better resolution of hyperfine structure is obtained at frequencies lower than X, *viz.*, at L(1.2 GHz) and S(2–4 GHz) bands. However, in our case, the classical approach of going from X to Q band was highly satisfying. Spectra presented here are from powdered crystalline samples and their mesophases (Figs. 4–6) and the EPR parameters are given in Table VI.

4.1. Studies in $C_n\text{Cu}$ System

Work was extended to cover $C_6\text{Cu}$, $C_7\text{Cu}$, $C_9\text{Cu}$ and $C_{12}\text{Cu}$ ($C_8\text{Cu}$ and $C_{10}\text{Cu}$ was reported before). $C_6\text{Cu}$ behaved as the prototype columnar one dimensional linear chain, as in $C_8\text{Cu}$ and gave the single highly asymmetric exchange-narrowed g_{\perp} line, along with a weak g_{\parallel} . $C_{12}\text{Cu}$ also showed a strongly exchange-narrowed asymmetric g_{\perp} line ($\Delta H \sim 20$ Oe) but the weak g_{\parallel} was so broad, that it was followed immediately by g_{\perp} . Interestingly, in the $C_n\text{Cu}$ series, there seems to be a sort of odd-even effect (Fig. 4a). Thus $C_7\text{Cu}$ and $C_9\text{Cu}$ show a different spectra *viz.*, g_{\parallel} is a well separated hyperfine quartet ($A_{\parallel} \sim 180$ Oe) for both, and g_{\perp} is still exchange-narrowed in $C_9\text{Cu}$ but not in $C_7\text{Cu}$. The g_{\perp} line-width of the interacting pair in Q band at room temperature is ~ 130 Oe in the former. Unfortunately for $C_9\text{Cu}$, which is rather unique in having three different mesophases, there is no crystal structure data. It also shows the copper hyperfine quartet in g_1 but g_{\perp} is now splitted up giving g_2 and g_3 . g_2 , which corresponds to g_{\perp} is also exchange-narrowed ($\Delta H \sim 25$ Oe) and g_3 is weak, showing that the system is non-axial and thus different from other members of the $C_n\text{Cu}$ series. The texture in the

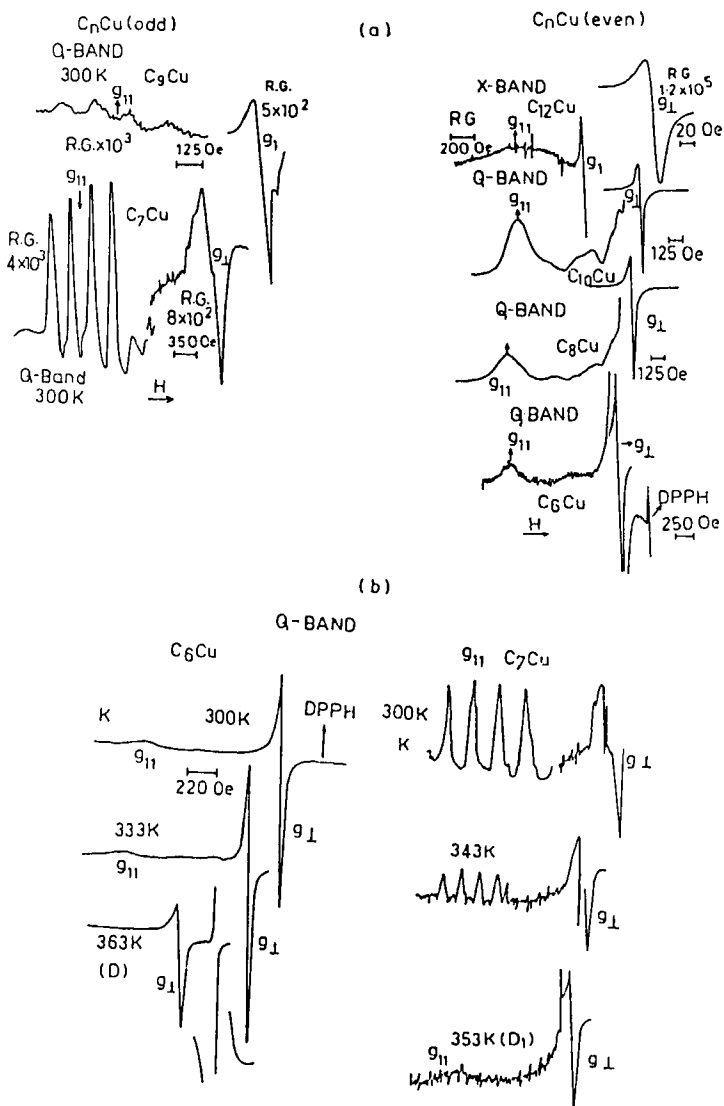


FIGURE 4 (a) Room temperature EPR spectra of $C_n\text{Cu}$: Odd $C_7\text{Cu}$ and $C_9\text{Cu}$, even $C_6\text{Cu}$, $C_8\text{Cu}$, $C_{10}\text{Cu}$ and $C_{12}\text{Cu}$; (b) Temperature variation studies of $C_6\text{Cu}$ and $C_7\text{Cu}$ in Q Band.

D_1 phase is spiral, which may possibly result from a helicoidal packing in the K phase, as has been observed in Hexa-hexyl-thiotriphenylene [22] and mosaic in D_2 , which wrinkles in D_3 .

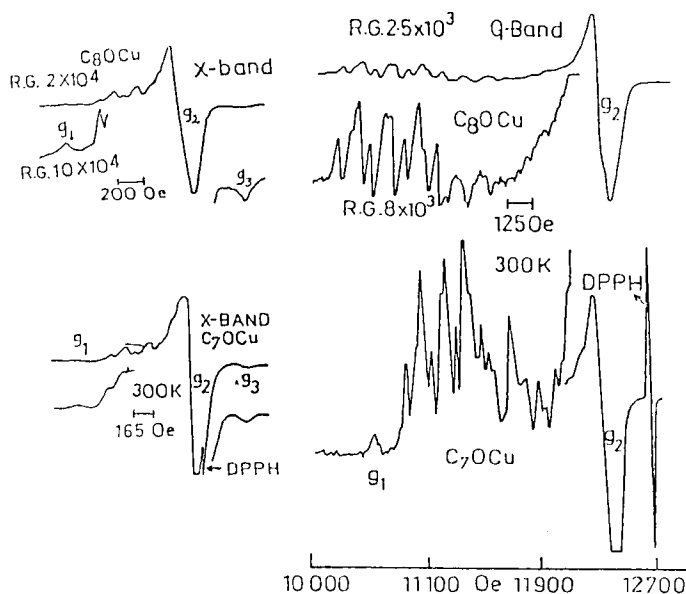


FIGURE 5 X/Q Band room temperature spectra of C_6OCu ; C_7OCu and C_8OCu .

4.2. Temperature Variation Studies in C_6Cu and C_7Cu

EPR spectra in Q band (Fig. 4b) are presented for C_6Cu/C_7Cu from K to the discotic phases. The exchange-narrowed g_{\perp} line in C_6Cu becomes wider (decreases in intensity) with increasing temperature and g_{\parallel} intensity also diminishes, till at the mesophase, g_{\parallel} almost vanishes. In C_7Cu the effects are striking. The quartet in the solid is slightly distorted but with temperature increasing, the distortion disappears and in the D_1 phase ($80^{\circ}C$) the quartet vanishes to give a weak g_{\parallel} . Thus g_{\perp} line narrows from 130 Oe in K phase to 50 Oe in D_1 . There is no significant change in the spectra from D_1 to D_2 phase ($100^{\circ}C$) except a marginal narrowing ($\Delta H \sim 45$ Oe) of g_{\perp} . However, in C_7Cu , the intermolecular interactions in the K phase is not so strong as in dimer C_8OCu . The weak nature of the interactions among adjacent neighbours is clearly shown up on heating. Thus at the mesophase, these interactions disappear (Fig. 4b), leading to the collapse of the hyperfine quartet, which is not the case in dimeric C_8OCu . Possibly, close packing in this phase leads to a larger exchange interaction, which is reflected in the narrowing of the g_{\perp} from 130 Oe to 50 Oe in C_7Cu . This is opposite to that in C_6Cu , where the exchange-narrowed line in K phase (30 Oe) increases to 60 Oe at $140^{\circ}C$ (mesophase).

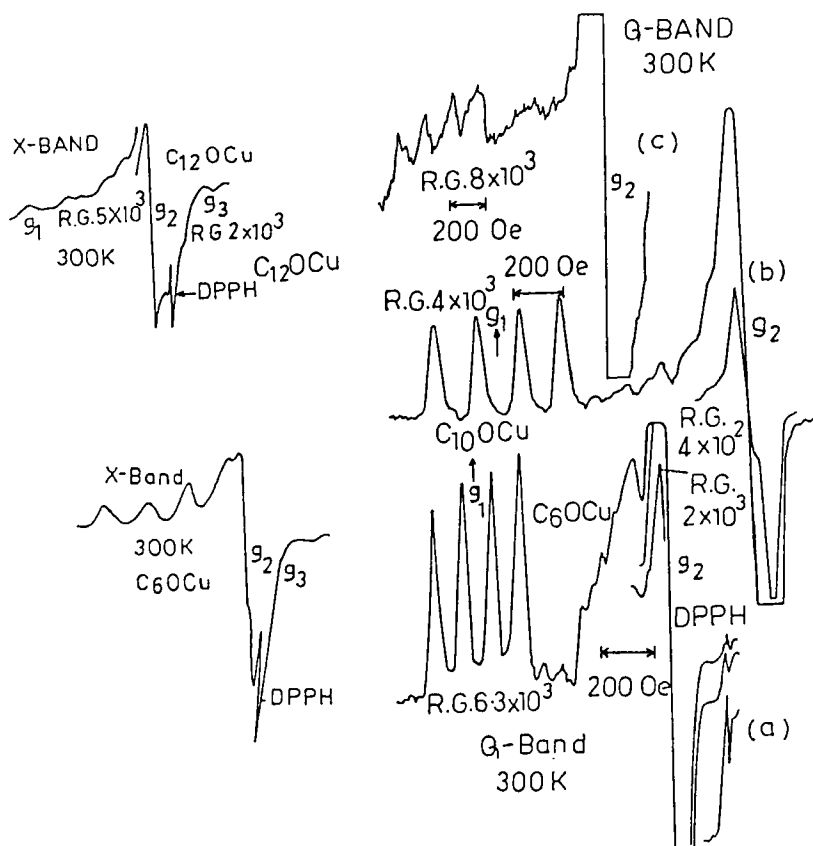


FIGURE 6 X/Q Band room temperature spectra of $C_n\text{OCu}$; $C_6\text{OCu}$, $C_{10}\text{OCu}$ and $C_{12}\text{OCu}$.

The difference in the behaviour of $C_6\text{Cu}$ (even) and $C_7\text{Cu}$ (odd) is also reflected in the dynamics of the two systems. Thus ^1H (proton) relaxation time T_1 at room temperature is very short in the exchange-narrowed $C_6\text{Cu}$ (~ 1.9 msec), comparable to T_1 in $C_8\text{Cu}$ (~ 2 msec), but very different from the rather long $T_1 \sim 68.9$ msec in $C_7\text{Cu}$ (unpublished work). However, T_1 has not been measured in $C_9\text{Cu}$.

4.3. Studies in $C_n\text{OCu}$ System

Detailed EPR studies on $C_8\text{OCu}$ has already been reported by us [18]. Computer-simulation has confirmed that the complex hyperfine structure

TABLE VI EPR parameters for C_nCu and C_nOCu complexes

C_nCu	Band	g_{\parallel} g_{\perp}	g_3	ΔH Oe	A_{\parallel} Oe	C_nOCu	Band	g_1	g_2	g_3	ΔH_{\perp} Oe	A_{\parallel} Oe
$C_6Cu(RT)$	Q	2.283	2.068	20		$C_6OCu(RT)$	Q	2.263	2.056		120	180
M		—	2.062	60			X	2.215	2.040	1.855	110	180
$C_7Cu(RT)$	Q	2.241	2.051	130	180	$C_7OCu(RT)$	Q	2.366	2.059		130	180
D_1		2.245	2.055	50			X	2.625	2.040	1.779	125	
D_2		2.245	2.055	45								
$C_8Cu(RT)$	Q	2.212	2.053	30		$C_8OCu(RT)$	X	2.55	2.060	1.78	140	
D_1		2.214	2.051	37.5		M		2.46	2.060	1.90	140	
D_2		2.215	2.050	40								
RT	X	2.243	2.069	20		RT	Q	2.377	2.252	—	140	
D_1		2.240	2.070	37.5		M		2.102	2.092		125	
D_2		2.240	2.070	40								
$C_9Cu(RT)$	Q	2.254	2.057	25	180							
$C_{10}Cu(RT)$	X	2.280	2.061	20		$C_{10OCu(RT)}$	Q	2.25	2.056		140	180
D		2.278	2.060									
RT	Q	2.380	2.061	30								
D	Q	2.382	2.059									
$C_{12}C_u(RT)$	X	2.49	1.886	20		$C_{12OCu(RT)}$	Q		2.054		80	180
						M			2.05		75	
						I			2.054		75	133
						RT	X	2.419	2.011	1.845	44	
tC_8Cu in C_8Pd	Q	2.258	2.138	2.03	180							
$^tC_{10}Cu$ in $C_{10}Pd$	Q	2.234	2.043	2.038	180							

ΔH_{\perp} = line width.
 A_{\parallel} = hyperfine interaction.
 M = Mesophase.
 I = Isotropic Phase.
 t = Ref. [19].

arises from overlapping Cu quartets and quadrupole forbidden transitions from $\Delta M_1 = \pm 1$ and ± 2 . Usha's X-ray studies [12] have shown that C_8OCu is a dimer, with no centre of inversion. In the present work, of the other C_nOCu complexes studied, only C_7OCu shows a complex hyperfine spectrum, very similar to that of C_8OCu . However, there is no X-ray data (no single crystal could be grown) to conclude that it is a dimer like C_8OCu . However, from the similarity in the EPR spectra of the two, it may not be unreasonable to infer that it is also in all possibility a dimer.

It may be pointed out that EPR spectra throughout the series is in harmony with the non-axial nature of C_nOCu . But C_6OCu , $C_{10}OCu$ and $C_{12}OCu$ exhibit only the Cu hyperfine (hf.) quartets but no quadrupolar forbidden transitions (q.f.t). For the first two, this quartet structure is in g_1 , but in $C_{12}OCu$, which is somewhat unique, the hf. quartet is in between g_1 and g_2 . However, g_2 lines for all three reveal weak or no exchange; asymmetries and line widths indicate, that exchange if present, is nowhere as strong as in the C_nCu series (Tab. VI). The absence of q.f.t. in these three, indicate that these are monomers with a more symmetrical structure, as compared to C_8OCu/C_7OCu . However, again there is no crystal structure data to support our contention.

Anisotropy is a primary criterion in liquid crystal formation and survey of the literature shows that the alkyl chain C_8H_{17} is possibly the most favoured chain in discotic and other liquid crystals. Possibly, this chain length is ideal for packing considerations, particularly, for the trans configuration of the chain in Ohta's model [6], based on C_8Cu . However, when $n > 8$, the trans configuration can lead to very loose packing of the molecules in the solid (thermodynamically not the lowest energy configuration), so that the conformation from $n > 8$ may be different. Thus the chains may be alternately up and down the core with a cis conformation, not only in $C_{12}OCu$, $C_{10}OCu$ and C_6OCu , but possibly in C_9OCu and $C_{11}OCu$. This structure has a high symmetry, compared to C_7OCu and C_8OCu , in which the trans alkyl chains in the plane of the core, leads to a highly asymmetric structure, responsible for the quadrupolar field gradient (q). For $n > 8$ (symmetric lamellar), with the higher symmetry, 'q' would tend to zero, so no q.f.t. are observed.

Further, temperature variation studies of $C_{12}OCu$ reveal that hyperfine quartets virtually disappear in the mesophase but reappears in the isotropic phase, albeit with a lower intensity and a somewhat smaller hyperfine interaction constant $A_{||}$. However, it has been pointed out that the quartets do not vanish in the mesophase of C_8OCu . Thus the collapse of the hyperfine quartet in the mesophase of $C_{12}OCu$, further supports our

contention that the chain conformation along with the packing is different from that of C_8OCu . This is also reflected in the shape of $C_{12}OCu$, which is needle like, being different from other rod or plate shaped members of C_nOCu series.

4.4. Effect of Frequency and Temperature on Line Widths (ΔH)

As g_{\parallel} lines in many cases are rather weak or split (quartet), one focusses on the g_{\perp} line-width. In the C_nCu series, the exchange-narrowed line-widths (ΔH) in $C_8Cu/C_{10}Cu$ are the same in the K phase viz., ~ 20 Oe in X band and ~ 30 Oe in Q band (Tab. VI). However, ΔH changes sharply in the mesophase due to disordering. For C_8Cu , ΔH values (~ 37.5 Oe in D_1 and ~ 40 Oe for D_2) are independent of frequency within experimental error. This is not the case in $C_{10}Cu$, as D has a value of ~ 35 Oe in X band but 60 Oe in Q band. Possibly, the exchange interaction in $C_{10}Cu$ is somewhat weaker than in C_8Cu . Thus as expected, in case of the exchange-narrowed lines in the crystalline phase, change of frequency strongly affects ΔH . Increasing the temperature, leads to the mesophases, wherein, ΔH is found to be much larger, as disordering affects exchange.

In C_8OCu , where ΔH is not exchange-narrowed, frequency seems to have no effect in the K phase, as both in X and Q bands, $\Delta H \sim 140$ Oe. Spin-spin interaction in C_8OCu dimer possibly determine ΔH . However, in the mesophase, the higher magnetic field in Q band (12,500 Oe) possibly breaks up the dimer, [15] as evidenced in the collapse of q.f.t. This shows a $\Delta H \sim 125$ Oe, whereas in the X band (3000 Oe), the hf. structure has just started to distort, but ΔH remains unaltered (~ 140 Oe).

Not unexpectedly, A_{\parallel} in the hyperfine quartet in both C_nCu and C_nOCu is almost constant (~ 180 Oe) within experimental error. This hf. interaction constant reflects the bonding situation in the CuO_4 core, which is essentially the same in these square planar complexes and is unaffected by the alkyl chain length, as also packing. Thus, even in dilute systems viz., $C_8Cu/C_{10}Cu$ doped in $C_8Pd/C_{10}Pd$ respectively, A_{\parallel} remains unchanged, as it is a molecular parameter.

5. CONCLUSIONS

EPR studies in C_nCu/C_nOCu series reveal basically three different spectral types in powders:

1. Single strongly exchange-narrowed asymmetric g_{\perp} line, along with a weak g_{\parallel} for C_6Cu , C_8Cu , $C_{10}Cu$ and $C_{12}Cu$ (even) but not for C_7Cu and C_9Cu (odd) in the columnar C_nCu series.
2. Normal hyperfine quartet for copper in g_1 with a single g_2 and a weak g_3 for C_6OCu and $C_{10}OCu$ but in between g_1 and g_2 in $C_{12}OCu$ in the lamellar C_nOCu series.
3. Hyperfine quartet with quadrupole forbidden transitions (q.f.t.) in between weak g_1 and the strong broad single g_2 , along with a weak g_3 in C_8OCu and C_7OCu . In C_8OCu , dimer formation (confirmed from X-ray) is possibly responsible for the forbidden transitions, which however vanish at the mesophase, but the quartet persists.
4. C_7Cu and C_9Cu in the C_nCu series are rather unique, as they do not exhibit a columnar structure. Both give a hyperfine quartet in g_{\parallel} . C_7Cu like C_8Cu , give two mesophases, but unlike the latter, do not give an exchanged-narrowed g_{\perp} , as molecular arrangement within the crystal is very different. Thus though $z = 1$ for both, interaction between two adjacent molecules in C_7Cu along end-chains, as also phenyl-phenyl interaction, cause them to behave as a pair in the crystalline state, instead of the linear Heisenberg chain in columnar C_8Cu . However, this interaction is weak and vanishes in the mesophase (unlike the dimeric C_8OCu), as manifested in the disappearance of the quartet to give a weak g_{\parallel} . C_9Cu is the only member which shows three mesophases and may have a helicoidal structure, at least, not the regular columnar structure of the C_nCu series. EPR spectra shows C_9Cu to be the only non-axial member in this series.

Thus X-ray and EPR studies indicate that within each series, some members exhibit anomalous behaviour *viz.*, C_7Cu and C_9Cu in C_nCu and C_7OCu/C_8OCu in C_nOCu . Further, weak or no exchange in C_7Cu is confirmed from the rather long proton (1H) relaxation time (NMR $T_1 \sim 68.9$ msecs.), as compared to the short relaxation time $T_1 \sim 1.9$ msecs. in the strongly exchange-narrowed C_6Cu . The above studies along with melting points and miscibility behaviour, indicate that chain length does play an important role in both the series but not in a linear fashion. Interestingly, all members of the C_nCu and C_nOCu studied so far [23] crystallise in the triclinic space group ($P\bar{1}$), which possibly satisfies the structural requirement for efficient packing.

Acknowledgements

Our thanks are due to Prof. S. Subramanian, Head, RSIC of IIT Madras for his kind cooperation, and to Dr. Srilekha Banerjee for her help during the analysis of the EPR spectra. Monisha Bose and C. K. Majumdar are grateful to the DST, Government of India for sanctioning the project on 'Metallomesogens'.

References

- [1] A. M. Giroud-Godquin and J. Billard, *Mol. Cryst. Liq. Cryst.*, **66**, 147 (1981).
- [2] A. M. Levelut, *J. Chim. Physique*, **80**, 149 (1983).
- [3] J. Billard, C. R. Acad. Sc. Paris, Series II, **299**, 905 (1984).
- [4] K. Ohta, A. Ishii, I. Yamamoto and K. Matsuzaki, *J. Chem. Soc. Commun.*, p. 1099 (1984).
- [5] K. Ohta, A. Ishii, H. Muroki, I. Yamamoto and K. Matsuzaki, *Mol. Cryst. Liq. Cryst.*, **116**, 299 (1985).
- [6] K. Ohta, H. Muroki, A. Takagi, K. Hatada, H. Ema, I. Yamamoto and K. Matsuzaki, *Mol. Cryst. Liq. Cryst.*, **140**, 131 (1986).
- [7] H. Sakashita, A. Nishitani, Y. Sumiya, H. Terauchi, K. Ohta and I. Yamamoto, *Mol. Cryst. Liq. Cryst.*, **163**, 211 (1988).
- [8] K. Ohta, Hiromitsu Muroki, Akira Takagi, Iwao Yamamoto and Kei Matsuzaki, *Mol. Cryst. Liq. Cryst.*, **135**, 247 (1986).
- [9] K. Usha and K. Vijayan, *Mol. Cryst. Liq. Cryst.*, **220**, 77 (1992).
- [10] A. M. Giroud-Godquin and J. Billard, *Mol. Cryst. Liq. Cryst.*, **97**, 287 (1983).
- [11] R. Fugnitto, H. Strzelecka, A. Zann, J. C. Dubois and J. Billard, *J. Chem. Soc. Chem. Comm.*, p. 271 (1980).
- [12] K. Usha and K. Vijayan, *Mol. Cryst. Liq. Cryst.*, **174**, 39 (1989).
- [13] M. P. Eastman, M. L. Horng, B. Freiha and K. W. Sheu, *Liq. Cryst.*, **2**, 223 (1987).
- [14] Monisha Bose and B. K. Sadashiva, *Mol. Cryst. Liq. Cryst. Letters*, **8**, 59 (1991).
- [15] Monisha Bose and B. K. Sadashiva, *Mol. Cryst. Liq. Cryst. Letters*, **8**, 137 (1992).
- [16] Monisha Bose, Jayashree Saha, Chanchal K. Majumdar and B. K. Sadashiva, *Mol. Cryst. Liq. Cryst.*, **307**, 43 (1997).
- [17] K. Usha, K. Vijayan and B. K. Sadashiva, *Mol. Cryst. Liq. Cryst.*, **201**, 13 (1991).
- [18] B. Bleaney, *Phil. Mag.*, **42**, 441 (1951).
- [19] Monisha Bose, Chanchal K. Majumdar and B. K. Sadashiva, *Mol. Cryst. Liq. Cryst.*, **307**, 57 (1997).
- [20] K. Usha, K. Vijayan, B. K. Sadashiva and P. R. Rao, *Mol. Cryst. Liq. Cryst.*, **185**, 1 (1990).
- [21] J. S. Hyde and W. Froncisz, *Ann. Rev. Biophys. Bioeng.*, **11**, 391 (1982).
- [22] E. Fontes, P. A. Heine and W. H. de Jeu, *Phys. Rev. Letters*, **61**, 1202 (1988).
- [23] K. Usha, K. Vijayan and S. Chandrasekhar, *Liq. Cryst.*, **15**, 575 (1993).